29 November 2001
PHYSICS LETTERS B
ELSEVIER
Physics Letters B 521 (2001) 243–251
www.elsevier.com/locate/npe

A possibility to measure CP-violating effects in the decay $K \to \mu\nu\gamma$

R.N. Rogalyov

Institute for High Energy Physics, Protvino, Russia

Received 4 June 2001; received in revised form 5 July 2001; accepted 29 August 2001
Editor: R.Gatto

Abstract

It is argued that a precise measurement of the transverse component of the muon spin in the decay $K \to \mu\nu\gamma$ makes it possible to obtain more stringent limits on CP-violating parameters of the leptoquark, SUSY and left–right symmetric models. The results of the calculations of the CP-even transverse component of the muon spin in the decay $K \to \mu\nu\gamma$ due to the final-state electromagnetic interactions are presented. The weighted average of the transverse component of the muon spin comprises $\sim 2.3 \times 10^{-4}$.

1. Introduction

The transverse component of the muon spin in the decay $K \to \mu\nu\gamma$ beyond the Standard Model is due to both the electromagnetic and CP- and T-violating interactions:

$$\xi = \xi_{\mathrm{EM}} + \xi_{\mathrm{odd}}, \tag{1}$$

where ξ_{EM} is the contribution of the electromagnetic Final-State Interactions (FSI) ξ_{odd} is the contribution of the CP-odd interactions.

Current limitations on the CP-violation parameters in various nonstandard models allow the transverse component of the muon spin in the decay $K \to \mu\nu\gamma$ to be rather large [1]: the left–right symmetric models based on the symmetry group $SU(2)_L \times SU(2)_R \times U(1)_{B-L}$ with one doublet Φ and two triplets $\Delta_{L,R}$ of Higgs bosons can give $\xi_{\mathrm{odd}} \sim 3.5 \times 10^{-3}$ [2], supersymmetric models—$\xi_{\mathrm{odd}} \sim 5 \times 10^{-3}$ [3], leptoquark models—$\xi_{\mathrm{odd}} \sim 2.5 \times 10^{-3}$ [4]. To extract the value of ξ_{odd} from the experimental data, one should know the value of ξ_{EM} exactly.

It has long been known that [5] the transverse polarization of the muon can be accounted for by the imaginary parts of the form factors parametrizing the expression for the amplitude of the decay. In this work, we compute the contribution of the electromagnetic FSI to the transverse component of the muon spin in the decay $K \to \mu\nu\gamma$ in the one-loop approximation (to be certain, we consider the decay $K^+ \to \mu^+\nu\gamma$). Our calculations are performed in the framework of the Chiral Perturbation Theory (ChPT) [6].

It should be mentioned that some contributions to ξ_{EM} were calculated in [8,9]. In contrast to the mentioned calculations, we take into account a complete set of the diagrams contributing to the imaginary part of the decay amplitude in the leading order of the ChPT.

For the description of decay $K^+(p_K) \to \mu^+(k) \times \nu(k')\gamma(q)$, we use the following variables: $M_K = 494$ MeV and $m_\ell = 106$ MeV are the kaon and muon

E-mail address: rogalyov@mx.ihep.su (R.N. Rogalyov).

0370-2693/01
PII: S0370-2693(01)01198-4

masses;

$$x = \frac{2p_K \cdot q}{M_K^2}, \qquad y = \frac{2p_K \cdot k}{M_K^2},$$
$$\lambda = \frac{1-y+\rho}{x}, \qquad \rho = \frac{m_\ell^2}{M_K^2}, \qquad \gamma = \frac{F_A}{F_V},$$
$$\tau = (1-\lambda)x + \rho, \qquad \zeta = 1-\lambda-\tau,$$
$$F_V = \frac{\sqrt{2}\,M_K}{8\pi^2 F}, \qquad F_A = \frac{4\sqrt{2}\,M_K(L_9+L_{10})}{F}; \quad (2)$$

$L_9 = 6.9 \pm 0.7 \times 10^{-3}$ and $L_{10} = -5.5 \pm 0.7 \times 10^{-3}$ are the parameters of the $O(p^4)$ ChPT Lagrangian; and $F = 93$ MeV. The relevant terms of the ChPT Lagrangian [6,7] have the form

$$\begin{aligned}
L_{\mathrm{CHPT}}^{K\to\mu\nu\gamma} = {} & F G_{\mathrm{F}} V_{\mathrm{us}} \partial_\mu K^+ l_\mu^- \\
& - e\bar{\mu}\hat{A}\mu + ieA_\mu \partial_\mu K^+ K^- \\
& + iG_{\mathrm{F}} e V_{\mathrm{us}}^* F K^- A_\mu l_\mu^+ \\
& - \frac{G_{\mathrm{F}} e V_{\mathrm{us}}^*}{F}\Bigg(\frac{1}{8\pi^2}\varepsilon^{\mu\nu\alpha\beta}\partial_\mu K^+ \partial_\alpha A_\nu l_\beta^- \\
& \qquad - 4\sqrt{2}\,iM_\pi(L_9+L_{10}) \\
& \qquad \times \partial_\mu K^+ l_\nu^-(\partial_\mu A_\nu - \partial_\nu A_\mu)\Bigg) \\
& - \frac{\alpha}{2\pi F}\varepsilon^{\mu\nu\alpha\beta}\partial_\mu A_\nu \partial_\alpha A_\beta \pi^0 \\
& + \frac{iG_{\mathrm{F}}}{2} V_{\mathrm{us}}^* l_\mu^-\big(K^+\partial_\mu \pi^0 - \pi^0 \partial_\mu K^+\big), \quad (3)
\end{aligned}$$

where $G_{\mathrm{F}} = 1.17 \times 10^{-5}\ \mathrm{GeV}^{-2}$ is the Fermi constant; $\alpha = e^2/(4\pi) = 7.3 \times 10^{-3}$, e is the electron charge; $V_{\mathrm{us}} = 0.22$ is the element of the Cabibbo–Kobayashi–Maskawa matrix; K^+, π^0, A, ν and μ are the fields of the K^+ meson, π^0 meson, photon, antineutrino, and muon, respectively; $l_\beta^+ = \bar{\mu}\gamma_\beta(1-\gamma^5)\nu$; $l_\beta^- = \bar{\nu}\gamma_\beta(1-\gamma^5)\mu$.

2. Expression for polarization of muon in terms of helicity amplitudes

Experimentally, the transverse component of the muon spin can be defined as follows:

$$\xi = \frac{N_+ - N_-}{2(N_+ + N_-)}, \tag{4}$$

where N_+ (N_-) is the number of the produced muons whose spin is directed along (against) a beforehand specified direction of polarization. We introduce vector $\vec{o}$ specifying such direction in the case under consideration. In the kaon rest frame, it is orthogonal to the vectors $\vec{q}, \vec{k}$, and $\vec{k}'$ (in this frame, these three vectors are linearly dependent):

$$\vec{\mathbf{o}} = \frac{2}{M_K^3 x\sqrt{\lambda\zeta}}\big(\vec{\mathbf{q}} \times \vec{\mathbf{k}}\big), \tag{5}$$

a positive value of ξ implies that the projection of spin of muon on vector $\vec{o}$ is positive: $\vec{s}\vec{o} > 0$.

The respective 4-vector is defined as the unit vector orthogonal to the vectors q, k, and k': [1]

$$o^\lambda = \frac{2}{M_K^3 x\sqrt{\lambda\zeta}}\varepsilon^{\mu\nu\rho\lambda}k'_\mu k_\nu q_\rho, \tag{6}$$

or, to put it differently,

$$o^\mu = \frac{\omega_-^\mu(k,k') - \omega_+^\mu(k,k')}{i\sqrt{2}}, \tag{7}$$

where the vectors $\omega_-^\mu(k,k')$ and $\omega_+^\mu(k,k')$ are defined by the relations

$$\begin{aligned}
\hat{\omega}_+(k,k') = {} & -\frac{\sqrt{2}}{2M_K^3 x\sqrt{\lambda\zeta}}\Bigg(\hat{k}\hat{q}\hat{k}'\big(1-\gamma^5\big) \\
& + \hat{k}'\hat{q}\hat{k}\big(1+\gamma^5\big) - \frac{2\rho x\lambda}{1-x-\rho}\hat{k}'\Bigg), \\
\hat{\omega}_-(k,k') = {} & -\frac{\sqrt{2}}{2M_K^3 x\sqrt{\lambda\zeta}}\Bigg(\hat{k}\hat{q}\hat{k}'\big(1+\gamma^5\big) \\
& + \hat{k}'\hat{q}\hat{k}\big(1-\gamma^5\big) - \frac{2\rho x\lambda}{1-x-\rho}\hat{k}'\Bigg).
\end{aligned} \tag{8}$$

The helicity amplitudes for the decay $K^+(p) \to \mu^+(k)\nu(k')\gamma(q)$ are defined as follows:

$$\mathcal{M}_{rs} = \big\langle \mu_s(k)\nu(k')\gamma_r(q)\big|\mathcal{M}\big|K(p)\big\rangle, \tag{9}$$

where $r = \pm$ is the helicity of the photon; $s = \pm$ is the helicity of the muon in the reference frame comoving with the center of mass of the muon and neutrino, and the amplitude $\mathcal{M}$ is defined by

$$S = 1 - (2\pi)^4 i\delta(k + k' + q - p)\mathcal{M},$$

where S is the scattering matrix in the respective channel.

[1] Here and below, $\epsilon^{0123} = -1$, $\mathrm{Tr}\,\gamma^5\gamma^\mu\gamma^\nu\gamma^\alpha\gamma^\beta = 4i\varepsilon^{\mu\nu\alpha\beta}$.

The particles produced in the decay $K \to \mu\nu\gamma$ can be described by the wave function

$$
\begin{aligned}
|\Psi\rangle &= S\big|K(p)\big\rangle \\
&= \frac{1}{\Gamma}\int d\Phi\,\big(\mathcal{M}_{--}\big|\gamma_-(q)\mu_-(k)\nu(k')\big\rangle \\
&\qquad + \mathcal{M}_{-+}\big|\gamma_-(q)\mu_+(k)\nu(k')\big\rangle \\
&\qquad + \mathcal{M}_{+-}\big|\gamma_+(q)\mu_-(k)\nu(k')\big\rangle \\
&\qquad + \mathcal{M}_{++}\big|\gamma_+(q)\mu_+(k)\nu(k')\big\rangle\big),
\end{aligned}
\tag{10}
$$

where Γ is the decay width, and the element of the phase space has the form

$$
d\Phi = \frac{1}{(2\pi)^5}\delta(k+k'+q-p)\frac{d^3\mathbf{k}}{2k_0}\frac{d^3\mathbf{k}'}{2k_0'}\frac{d^3\mathbf{q}}{2q_0}.
$$

The operator of spin s_μ acts on fermion states as follows:

$$
s_\mu = \frac{W_\mu}{m} = -\frac{\gamma_\mu\gamma^5}{2}\hat{\varepsilon}_0, \tag{11}
$$

where W_μ is the Pauli–Lubanski vector and $\hat{\varepsilon}_0$ is the operator of the sign of energy. The average value of the transverse component of spin in the state $|\Psi\rangle$ is equal to $\langle\Psi|(-s_\mu\cdot o_\mu)|\Psi\rangle$.

Since

$$
\begin{aligned}
\big\langle\mu_-(\vec{k})\big|s^\nu\big|\mu_-(\vec{k})\big\rangle &= -\frac{1}{4m_\ell}\bar{v}(k,N)\gamma^\nu\gamma^5 v(k,N) \\
&= \frac{N^\nu}{2}, \\
\big\langle\mu_-(\vec{k})\big|s^\nu\big|\mu_+(\vec{k})\big\rangle &= -\frac{1}{4m_\ell}\bar{v}(k,-N)\gamma^\nu\gamma^5 v(k,N) \\
&= -\frac{\omega_-^\nu}{\sqrt{2}}, \\
\big\langle\mu_+(\vec{k})\big|s^\nu\big|\mu_-(\vec{k})\big\rangle &= -\frac{1}{4m_\ell}\bar{v}(k,N)\gamma^\nu\gamma^5 v(k,-N) \\
&= -\frac{\omega_+^\nu}{\sqrt{2}}, \\
\big\langle\mu_+(\vec{k})\big|s^\nu\big|\mu_+(\vec{k})\big\rangle &= -\frac{1}{4m_\ell}\bar{v}(k,-N)\gamma^\nu\gamma^5 v(k,-N) \\
&= -\frac{N^\nu}{2},
\end{aligned}
\tag{12}
$$

where spinor $v(k,N)$ describes the muon of momentum k and vector of spin N,

$$
N_\nu = \frac{(1-x-\rho)k_\nu - 2\rho k_\nu'}{m_\ell(1-x-\rho)}, \tag{13}
$$

the expectation value of the transverse component of the muon spin is determined by the relation

$$
\begin{aligned}
\xi = \frac{\Xi}{\mathcal{N}^2} \equiv \frac{1}{\mathcal{N}^2}\big(&\mathcal{M}'_{--}\mathcal{M}''_{-+} - \mathcal{M}'_{-+}\mathcal{M}''_{--} \\
&+ \mathcal{M}'_{+-}\mathcal{M}''_{++} - \mathcal{M}'_{++}\mathcal{M}''_{+-}\big),
\end{aligned}
\tag{14}
$$

where $\mathcal{N}$ is the normalization factor,

$$
\mathcal{N}^2 = \sum_{i,j=\pm}|\mathcal{M}_{i,j}|^2;
$$

$$
\mathcal{M}_{r,s} = \mathcal{M}'_{r,s} + i\mathcal{M}''_{r,s} \quad (r,s=\pm)
$$

(this formula is readily obtained by isolating an infinitesimal volume of the phase space of the particles produced in the decay and employing formula (10)).

In the calculations of the helicity amplitudes, we use the so-called diagonal spin basis [10–12] formed by the vectors $\omega_\pm^\mu$ and light-like linear combinations of the vectors k and k'.

With the use of this basis, the helicity amplitude $\mathcal{M}_{r,s}$ can be represented in a manifestly covariant form:

$$
\begin{aligned}
\mathcal{M}_{r,s} &= \bar{u}(k')\mathcal{M}_\alpha(k,k',q)\epsilon_\alpha(r)v(k,sN) \\
&= \mathrm{Tr}\,\mathcal{M}_\alpha(k,k',q)\epsilon_\alpha(r)v(k,sN)\bar{u}(k'),
\end{aligned}
\tag{15}
$$

where the expression for $\mathcal{M}_\alpha(k,k',q)$ is given by the Feynman diagrams, the polarization vectors of the photon are equal to

$$
\begin{aligned}
\epsilon_\mu(\pm) = \frac{\sqrt{2}}{2M_K x\sqrt{\lambda\zeta}}\bigg(&-x\lambda k_\mu + x(1-\lambda)k'_\mu \\
&- (1-\rho-x)q_\mu \\
&\mp \frac{2i}{M_K^2}\varepsilon_{kk'q\mu}\bigg),
\end{aligned}
\tag{16}
$$

and the quantities $v(k,sN)\bar{u}(k')$ can be brought in the form

$$
\begin{aligned}
v_\mu(k,-N)\bar{u}_\nu(k') &= \frac{(\hat{k}-m_\ell)\hat{k}'}{2M_K\sqrt{1-x-\rho}}\big(1+\gamma^5\big), \\
v_\mu(k,N)\bar{u}_\nu(k') &= \frac{M_K^2(1-x-\rho) - m_\ell\hat{k}'}{2M_K\sqrt{1-x-\rho}}\hat{\omega}_- \\
&\quad\times\big(1+\gamma^5\big).
\end{aligned}
\tag{17}
$$

The leading contribution to the real part of the decay amplitude is given by the tree diagrams corresponding

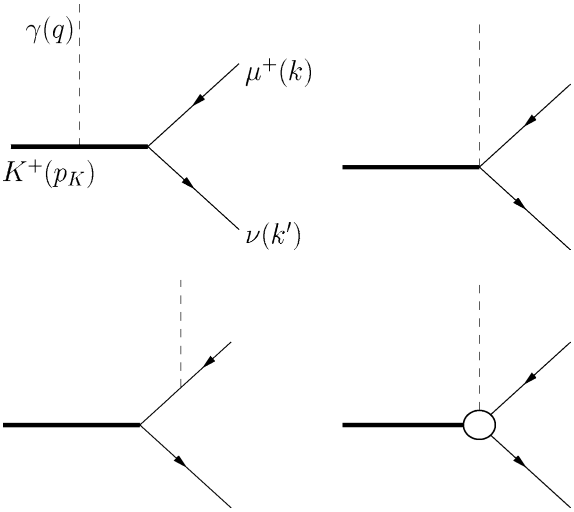

Fig. 1. Diagrams describing the decay $K \to \mu\nu\gamma$ in the tree approximation.

to Lagrangian (3) [7] (see Fig. 1). The helicity amplitudes for the decay $K^+ \to \mu^+\nu\gamma$ in the tree approximation have the form

$$\begin{aligned}
\mathcal{M}_{--} &= 2iG_{\mathrm{F}}eV_{\mathrm{us}}^* m_\ell x \frac{\sqrt{\lambda\zeta}}{1-x-\rho} \\
&\quad \times \left(\frac{\sqrt{2}\,F(1-\rho)}{x^2(1-\lambda)} - M_K \frac{F_V - F_A}{2}\right), \\
\mathcal{M}_{-+} &= -2iG_{\mathrm{F}}eV_{\mathrm{us}}^* \frac{x\lambda}{\sqrt{1-x-\rho}} \\
&\quad \times \left(m_\ell F \frac{\sqrt{2\rho}}{x(1-\lambda)} - \frac{F_V - F_A}{2} M_K^2 (1-x)\right), \\
\mathcal{M}_{+-} &= 2iG_{\mathrm{F}}eV_{\mathrm{us}}^* m_\ell x \sqrt{\frac{\lambda\zeta}{1-x-\rho}} \\
&\quad \times \left(F \frac{\sqrt{2}\,(1-x-\rho)}{x^2(1-\lambda)} + \frac{F_V + F_A}{2} M_K\right), \\
\mathcal{M}_{++} &= iG_{\mathrm{F}}eV_{\mathrm{us}}^* \frac{(F_V + F_A)x}{\sqrt{1-x-\rho}} M_K^2 \zeta, \qquad (18)
\end{aligned}$$

where the first index in the left-hand side denotes the polarization of the photon and the second—the polarization of the muon in the reference frame comoving with the center-of-mass of the lepton pair. The calculation of the imaginary parts of the helicity amplitudes is considered in the following section.

The differential probability for the decay is determined by the matrix element squared

$$\begin{aligned}
\sum_{\text{polariz.}} |\mathcal{M}|^2 &= \left|G_{\mathrm{F}}eV_{\mathrm{us}}^*\right|^2 \\
&\quad \times \left(m_\ell^2 F^2 IB + \frac{(F_V + F_A)^2}{2M_K^2} SD_+ \right. \\
&\qquad + \frac{(F_V - F_A)^2}{2M_K^2} SD_- + m_\ell F \frac{F_V + F_A}{\sqrt{2}\,M_K} INT_+ \\
&\qquad \left. + m_\ell F \frac{F_V - F_A}{\sqrt{2}\,M_K} INT_-\right), \qquad (19)
\end{aligned}$$

where

$$\begin{aligned}
IB &= \frac{8\lambda}{x^2(1-\lambda)} \\
&\quad \times \left(x^2 + 2(1-x)(1-\rho) - \frac{2\rho(1-\rho)}{1-\lambda}\right), \\
SD_+ &= 2M_K^6 x^2 (1-\lambda)\zeta, \\
SD_- &= 2M_K^6 x^2 \lambda\big((1-x)\lambda + \rho\big), \\
INT_+ &= \frac{8M_K^2 m_\ell \lambda}{1-\lambda}\zeta, \\
INT_- &= -\frac{8M_K^2 m_\ell \lambda}{1-\lambda}(1 - \lambda + \lambda x - \rho). \qquad (20)
\end{aligned}$$

3. Contribution of FSI to imaginary part of decay amplitude

The imaginary part of the amplitude for the decay $K \to \mu\nu\gamma$ in the leading order of the perturbation theory is described by the diagrams in Fig. 2. We take into account the diagrams in Figs. 2g and 2h omitted by the authors of [8] in spite of the fact that they are of the same order of magnitude.

We employ the Cutkosky rules [13] to replace the propagators with the δ functions. Thus we obtain the expression for the imaginary part of the amplitude in terms of the integrals:

$$\begin{aligned}
\mathcal{M}_i'' &= \frac{\alpha F}{2\pi} G_{\mathrm{F}}eV_{\mathrm{us}}^* \int dr\, \frac{\Delta}{N_i(r\cdot q, r\cdot k)} \bar{u}(k')\big(1+\gamma^5\big) \\
&\quad \times T_i(r, k, k', q, \epsilon) v(k), \qquad (21)
\end{aligned}$$

where N_i is the product of the remaining propagators in the respective diagram and T_i are the respective tensor structures (label i specifies the diagram in

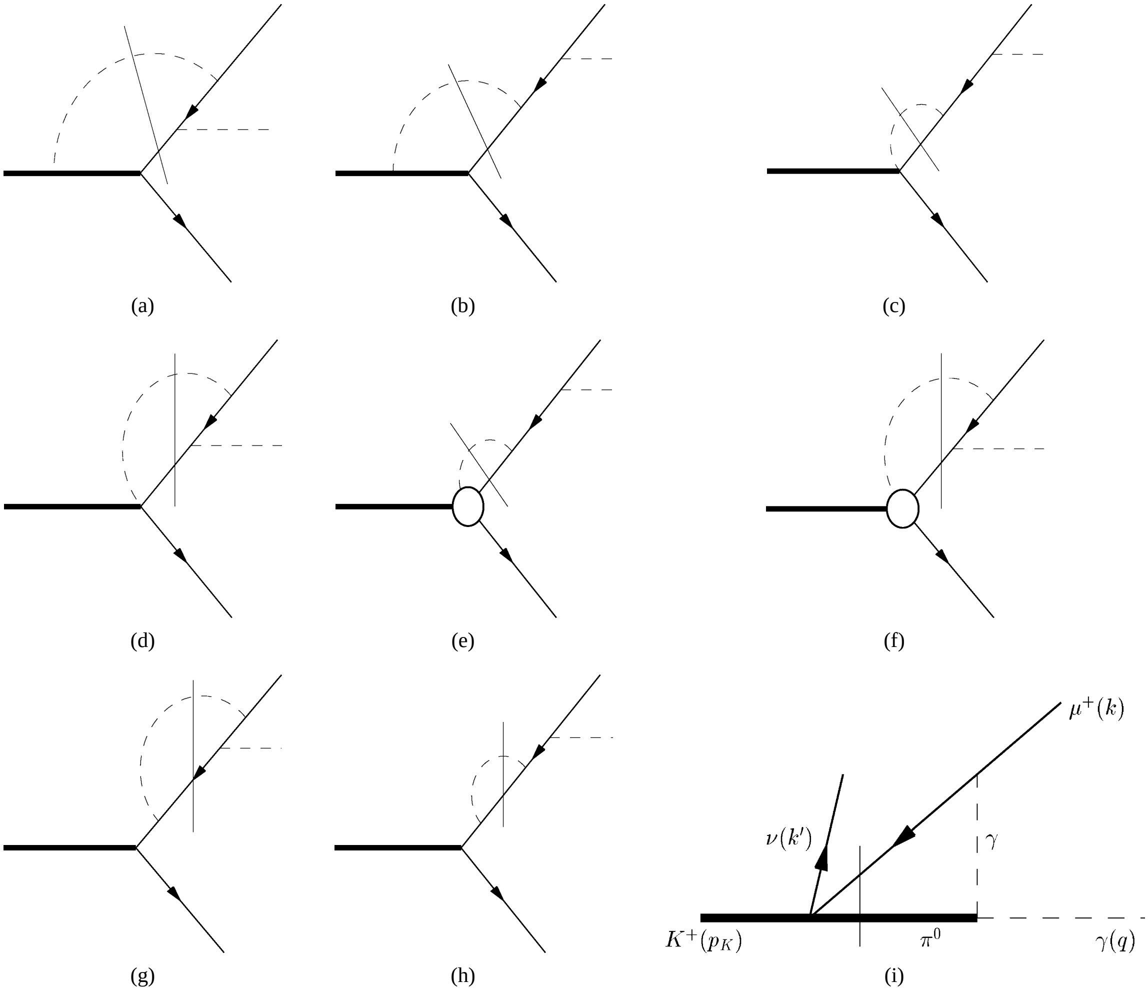

Fig. 2. Diagrams giving a contribution to the imaginary part of the amplitude of the decay $K \to \mu\nu\gamma$.

Fig. 2, $i =$ a–i); in the case of the diagrams a–h in Fig. 2, $\Delta = \delta(r^2 - m_\ell^2)\delta((k+q-r)^2)$ whereas, for the diagram in Fig. 2i, $\Delta = \delta((r+q)^2 - M_\pi^2) \times \delta((k-r)^2 - m_\ell^2)$ ($M_\pi = 135$ MeV—is the mass of the π^0 meson).

The computations of the diagrams in Fig. 2 are made with the *REDUCE* package. These diagrams are calculated exactly, no approximation is used.

The calculated imaginary part of the amplitude of the decay $K \to \mu\nu\gamma$ takes the form

$$\mathcal{M}'' = \frac{G_F e V_{us}^*}{4\pi} \bar{u}_\nu(k')\left(1+\gamma^5\right) \times \left(\mathcal{M}^{IB} + \mathcal{M}^{SD} + \mathcal{M}^{(\pi)}\right) v_\mu(k), \qquad (22)$$

where

$$\mathcal{M}^{IB} = \frac{2\pi\alpha F}{M_K^2} \sum_{n=1}^{4} c_n^{IB} \mathcal{E}_n \qquad (23)$$

is the contribution of the diagrams in Figs. 2a, 2b, 2c, 2d, 2g and 2h;

$$\mathcal{M}^{SD} = \frac{\pi\sqrt{2}\alpha}{M_K} \sum_{n=1}^{4} \left(-F_A c_n^A + F_V c_n^V\right) \mathcal{E}_n \qquad (24)$$

is the contribution of the diagrams in Figs. 2e and 2f and

$$\mathcal{M}^{(\pi)} = \frac{\alpha}{4\pi F}\big(c_2^{(\pi)}\mathcal{E}_2 + c_4^{(\pi)}\mathcal{E}_4\big) \tag{25}$$

is the contribution of the diagram in Fig. 2i. Tensor structures $\mathcal{E}_i$ have the form

$$\begin{aligned}
\mathcal{E}_1 &= M_K^2 m_\ell x\big[(1-\lambda)k'\cdot\epsilon - \lambda k\cdot\epsilon\big],\\
\mathcal{E}_2 &= M_K^2\left[k\cdot\epsilon\hat{q} - \frac{M_K^2}{2}x(1-\lambda)\hat{\epsilon}\right],\\
\mathcal{E}_3 &= M_K^2\left[k'\cdot\epsilon\hat{q} - \frac{M_K^2}{2}x\lambda\hat{\epsilon}\right],\\
\mathcal{E}_4 &= M_K^2 m_\ell\hat{q}\hat{\alpha},
\end{aligned} \tag{26}$$

and the coefficients in the above expressions are given by

$$\begin{aligned}
c_1^{IB} &= -\frac{4}{(1-\lambda)x}\big(G_3 - (1+\tau)G_2 + \rho(F_1 - F_2)\big),\\
c_2^{IB} &= \frac{4\rho}{(1-\lambda)x}\big(2G_1 + (1+\tau)G_2 - (1-\tau)G_3\\
&\qquad - (\tau+\rho)F_1\big) + 2F_5\rho,\\
c_3^{IB} &= 4\rho(-F_2 - G_4),\\
c_4^{IB} &= \frac{2\lambda}{(1-\lambda)}(G_3 - G_2 - \rho F_2) - 2(G_2 + 2G_1 - F_1)\\
&\quad + \frac{4 - x(1-\lambda)}{(1-\lambda)x}\big(2G_1 + G_2\\
&\qquad - (1-\tau)G_3 - \rho F_3\big)\\
&\quad + \frac{2}{(1-\lambda)}(-\tau F_1 + \rho F_3) - F_4 + F_5\rho,
\end{aligned} \tag{27}$$

$$\begin{aligned}
c_1^V &= \left(\frac{1}{3}x(1-\lambda) - 2\tau\right)F_5 + (\tau+\rho)F_6,\\
c_2^V &= \frac{1}{3}\big(\tau(1+5\tau-14\rho) - \rho(1-3\rho+x\lambda)\big)F_5\\
&\quad + \rho(\lambda x + 2\rho)F_6 + (1-\tau)F_7 - \frac{(1+\lambda)}{(1-\lambda)}F_8,\\
c_3^V &= -x(1-\lambda)\left(\tau + \frac{\rho}{3}\right)F_5 - \tau F_7 + F_8,\\
c_4^V &= \frac{1}{2}\Big(x\big(x(1-\lambda)^2 + \tau(3-2\lambda)\big)F_5\\
&\quad + x\big(1 - x - \lambda + \lambda x + \rho(3\lambda-4)\big)F_6\\
&\quad + (1-\tau)F_7\Big),\\
c_1^A &= c_1^V,\\
c_2^A &= c_2^V + 2\left(-\left(\frac{5x^2(1-\lambda)^2}{3} - \rho^2\right)F_5\right.\\
&\qquad\left. + \rho(x - x\lambda - \rho)F_6 + \tau F_7\right),\\
c_3^A &= c_3^V,\\
c_4^A &= c_4^V + \frac{1}{2}\big(-x(1-\lambda)\big(\tau + 2x(1-\lambda)\big)F_5\\
&\qquad + 4\rho x(1-\lambda)F_6 + 3\tau F_7\big),
\end{aligned} \tag{28}$$

$$\begin{aligned}
c_2^{(\pi)} &= \frac{1}{4M_K^2x^2(1-\lambda)^2}\theta\left(x - \frac{\kappa + \sqrt{2\kappa\rho}}{1-\lambda}\right)\\
&\quad\times\left(\frac{2\kappa^2\rho}{x(1-\lambda)}S_4 + \left(\big(x^2(1-\lambda)^2 - \rho\kappa\big)\right.\right.\\
&\quad\left.\left.\times\left(\frac{x(1-\lambda)}{\tau} + 2\right) + x^2(1-\lambda)^2\right)\frac{S}{\tau}\right),\\
c_4^{(\pi)} &= \frac{1}{4M_K^2x^2(1-\lambda)^2}\theta\left(x - \frac{\kappa + \sqrt{2\kappa\rho}}{1-\lambda}\right)\\
&\quad\times\left(\frac{\kappa^2(2\tau+\rho)}{x(1-\lambda)}S_4\right.\\
&\qquad + \left(\big(x^2(1-\lambda)^2 - \rho\kappa\big)\left(\frac{x(1-\lambda)}{\tau} + 3\right)\right.\\
&\qquad\left.\left. - 3\kappa\big(x(1-\lambda) + \tau\big)\right)\frac{S}{2\tau}\right),
\end{aligned} \tag{29}$$

where

$$\kappa = \frac{M_\pi^2}{M_K^2}; \tag{30}$$

θ function in formula (29) isolates the kinematic domain in which the imaginary part of the diagram in Fig. 2i does not vanish;

$$\begin{aligned}
S_1 &= \ln\left[1 + \frac{(1-\lambda)x}{\rho}\right],\\
S_2 &= \ln[\rho],\\
S_3 &= \ln\left[\frac{1 - \lambda x + \rho + \sqrt{R}}{1 - \lambda x + \rho - \sqrt{R}}\right],\\
S_4 &= \ln\left[\frac{(1-\lambda)x(\kappa - (1-\lambda)x + S) + 2\kappa\rho}{(1-\lambda)x(\kappa - (1-\lambda)x - S) + 2\kappa\rho}\right],
\end{aligned} \tag{31}$$

$$F_0 = \frac{1}{2M_K^2(1-\tau)x}\left(1 - \frac{\rho}{\tau} + \frac{1-\rho}{1-\tau}(S_1 + S_2)\right),$$

$$F_1 = \frac{1}{4M_K^2 x\zeta}\left(-2S_1 - S_2 + \frac{1-\lambda x+\rho}{\sqrt{R}}S_3 - \frac{2\rho}{(1-\lambda)\sqrt{R}}S_3\right),$$

$$F_2 = \frac{1}{4M_K^2 \lambda x\zeta}\left(\frac{2\lambda}{1-\tau}S_1 - \frac{\zeta-\lambda}{1-\tau}S_2 - \frac{\zeta-\lambda+x}{\sqrt{R}}S_3\right),$$

$$F_3 = \frac{1}{2M_K^2(1-\lambda)x\sqrt{R}}S_3,$$

$$F_4 = \frac{1}{M_K^2(1-\lambda)^2x^2}\big((1-\lambda)x - \rho S_1\big),$$

$$F_5 = \frac{1}{2M_K^2\tau^2},$$

$$F_6 = \frac{1}{M_K^2 x(1-\lambda)}\left(\frac{S_1}{x(1-\lambda)} - \frac{1}{\tau}\right),$$

$$F_7 = \frac{-x(1-\lambda)}{6M_K^2\tau^3}(x - x\lambda + 3\rho),$$

$$F_8 = \frac{\rho}{M_K^2 x(1-\lambda)}\left(\frac{x-x\lambda+2\rho}{x(1-\lambda)}S_1 - 2\right), \tag{32}$$

$$G_1 = \frac{1}{8M_K^2\lambda x\zeta}\left(\frac{2\lambda}{(1-\tau)}(\rho-\tau^2)S_1 + \frac{1-\lambda}{1-\tau}(1-2\rho-x-\tau x+\tau^2)S_2 + (1-\lambda)\sqrt{R}\,S_3\right),$$

$$G_2 = \frac{1}{\zeta}\big(-\lambda\rho F_3 + 2\lambda G_1 - (1-\tau)F_0\big),$$

$$G_3 = \frac{1}{\zeta}(-\rho F_3 + 2G_1 - F_0),$$

$$G_4 = \frac{1}{\lambda x}\big(-2G_1 + \tau(G_2 - F_1) + \rho(F_3 - F_1)\big). \tag{33}$$

Substituting expressions (22)–(29) in formula (14), we represent the transverse muon polarization in the form

$$\xi_{\rm EM} = \sum_{n=1}^{4} c_n Y_n \Big/ \sum_{r,s=\pm} |\mathcal{M}_{r,s}|^2, \tag{34}$$

where

$$c_n = \frac{\alpha}{4}\frac{G_{\rm F} e V_{\rm us}^*}{M_K^2}\left(2Fc_n^{IB} + \sqrt{2}\,M_K\big(c_n^V F_V - c_n^A F_A\big) + \frac{M_K^2}{4\pi^2 F}c_n^{(\pi)}\right), \tag{35}$$

$$Y_n = \bar{u}(k')\big(1+\gamma^5\big)\mathcal{E}_n^\alpha \times\Big(\epsilon_\alpha^-(q)\big(\mathcal{M}'_{-,-}v_+(k) - \mathcal{M}'_{-,+}v_-(k)\big) + \epsilon_\alpha^+(q)\big(\mathcal{M}'_{+,-}v_+(k) - \mathcal{M}'_{+,+}v_-(k)\big)\Big), \tag{36}$$

$v_\pm(k) = v(k, \pm N)$. Since the imaginary parts of the amplitudes under consideration are much less than the respective real parts ($\mathcal{M}''_{r,s} \ll \mathcal{M}'_{r,s}$), the denominator of expression (34) is determined by (19). The coefficients c_n^{IB}, c_n^V, c_n^A, $c_2^{(\pi)}$, and $c_4^{(\pi)}$ are given in formulas (27)–(29); $c_1^{(\pi)} = c_1^{(\pi)} = 0$; and

$$Y_1 = \frac{G_{\rm F} e V_{\rm us}^* m_\ell M_K^3\sqrt{2\lambda\zeta}}{1-\lambda} \times\big(M_K x^2(1-\lambda)\big((F_V - F_A)(1-x-\rho) + 2F_A\zeta\big) - 2\sqrt{2}F\rho\lambda\big),$$

$$Y_2 = \frac{G_{\rm F} e V_{\rm us}^* m_\ell M_K^3\sqrt{2\lambda\zeta}}{1-\lambda} \times\big(M_K x^2\lambda(1-\lambda)(F_V - F_A) + 2\sqrt{2}F(-\zeta+\lambda\rho)\big),$$

$$Y_3 = \frac{G_{\rm F} e V_{\rm us}^* m_\ell M_K^3\sqrt{2\lambda\zeta}}{1-\lambda} \times\big(M_K x^2\lambda(1-\lambda)(F_A - F_V) + 2\sqrt{2}F\lambda(1-\rho)\big),$$

$$Y_4 = \frac{G_{\rm F} e V_{\rm us}^* m_\ell M_K^3\sqrt{2\lambda\zeta}}{1-\lambda} \times\big(2M_K x^2\lambda(1-\lambda)(F_A - F_V) - 4\sqrt{2}F\lambda\rho\big). \tag{37}$$

4. Discussion of results and conclusion

The transverse component of the muon spin in the decay $K \to \mu\nu\gamma$ is plotted in Figs. 3 and 4 as a function of the kinematic variables x and y. As is seen, it varies through the range 0–$(-7) \times 10^{-4}$ and the the weighted average is equal to (the notation see

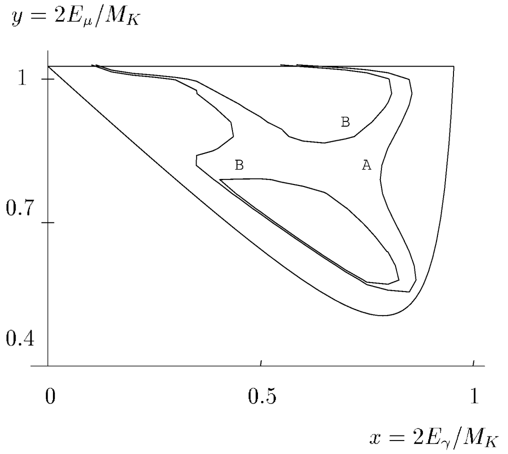

Fig. 3. Contour plot for the transverse spin $\xi_{\rm EM}$. Curve A: $\xi_{\rm EM} = -2.5 \times 10^{-4}$; curve B: $\xi_{\rm EM} = -5 \times 10^{-4}$.

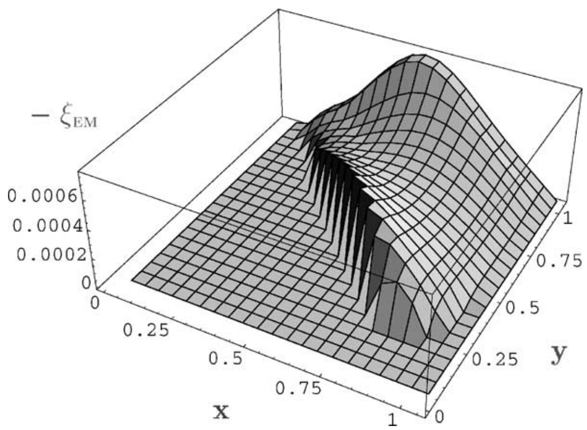

Fig. 4. The electromagnetic contribution to the transverse component of the muon spin over the Dalitz plot for the decay $K \to \mu\nu\gamma$.

in formula (14),

$$\langle \xi_{\rm EM} \rangle = \frac{\int_{x_{\min}} dx \int dy\, \Xi}{\int_{x_{\min}} dx \int dy\, \mathcal{N}^2} \sim 2.3 \times 10^{-4}, \qquad (38)$$

where the lower limit of the integration with respect to x, $x_{\min} = 0.1$, corresponds to the cutoff energy of the photon ~ 25 MeV. The accuracy of the result $\sim 20\%$ is determined by the accuracy of the ChPT in order $O(p^4)$ at these energies. Note that $\xi_{\rm EM}$ is negative in sign over all Dalitz plot (positive direction is given by the vector $\vec{o}$ introduced in Section 2).

The values of the parameters F_V and F_A used in our plots are $F_A = 0.042$ and $F_V = 0.095$; these values predicted by CHPT coincide with those used in [8,17].

The range of variation of the transverse polarization (which is twice the muon spin) agree with the results presented recently [17] and disagree with [8] and [9]. The point is that the authors of [8,9] took into account only a part of the diagrams contributing to the transverse polarization of the muon. Our results show that the diagram estimated in [9] does not give a leading contribution to the imaginary part of the amplitude and the maximum value of the transverse polarization of the muon is overestimated in [8] by an order of magnitude. However, it should be emphasized that our results sustantiate the conclusion made in [9]: "An experimental evidence of $P_T = 2\xi$ at the level of 10^{-3} would be a clear signal of physics beyond the SM,"—in spite of the fact that the analysis performed in [9] is incomplete. Our results contradict to the conclusion of [8].

And, finally, we note that our average value of ξ at the cutoff energy of the photon ~ 25 MeV agrees well with that presented in [17] despite the spectra are slightly different. The difference between the spectra may be due to instabilities in the computer program used by the authors of [17] for numerical computations.

Thus an observation of the transverse spin of the muon of the order 10^{-3} in the experiments [14–16] would signal CP and T violation because the background CP-even effect does not exceed 7×10^{-4} and its average value is not over 3×10^{-4}. Experiments of this sort can be a good tool for testing the above-mentioned nonstandard models.

Acknowledgements

I am grateful to A.E. Chalov, V.V. Braguta, and A.A. Likhoded for the interest in the study.

References

[1] C.H. Chen, C.Q. Geng, C.C. Lih, hep-ph/9709447.
[2] G. Barenboim et al., Phys. Rev. D 55 (1997) 4213.
[3] G.-H. Wu, J.N. Ng, hep-ph/9610533.
[4] G. Belanger, C.Q. Geng, Phys. Rev. D 44 (1991) 2789.
[5] L.B. Okun', I.B. Khriplovich, Yad. Fiz. 6 (1967) 821.
[6] J. Gasser, H. Leutwyler, Nucl. Phys. B 250 (1985) 465;

A. Pich, Rep. Prog. Phys. 58 (1995) 563.
[7] J. Bijnens et al., in: L. Maiani, N. Pancheri, N. Paver (Eds.), The Second DAΦNE Physics Handbbok, SIS, Frascati, 1995.
[8] V.P. Efrosinin, Yu.G. Kudenko, Phys. At. Nucl. 62 (1999) 987.
[9] G. Hiller, G. Isidori, Phys. Lett. B 459 (1999) 295.
[10] M.V. Galynskii et al., Zh. Eksp. Teor. Fiz. 95 (1989) 1921.
[11] A.A. Bogush et al., in: Proc. of the XI Workshop on High Energy Physics and Field Theory, Protvino, 1988;
R.N. Rogalyov, Teor. Mat. Fiz. 101 (1994) 384;
R.N. Rogalyov, Int. J. Mod. Phys. A 11 (1996) 3711.
[12] V.I. Borodulin, R.N. Rogalyov, S.R. Slabospitsky, hep-ph/9507456.
[13] C. Itzykson, J.-B. Zuber, Quantum Field Theory, McGraw-Hill, 1980.
[14] Yu.G. Kudenko, A. Khotyantsev, Phys. At. Nucl. 63 (2000) 820.
[15] V.F. Obraztsov, L.G. Landsberg, hep-ex/0011033.
[16] M. Abe et al., Phys. Rev. Lett. 83 (1999) 4253;
Yu.G. Kudenko, hep-ex/0103007.
[17] V.V. Braguta, A.A. Likhoded, A.E. Chalov, hep-ph/0105111.